

# Active antimicrobial extruded films for mozzarella cheese from poly (butylene adipate co-terephthalate) (PBAT) and orange oil

Michelle Félix de Andrade<sup>1\*</sup> , Ivo Diego de Lima Silva<sup>1</sup> , Viviane Fonseca Caetano<sup>1</sup> , Gisely Alves da Silva<sup>2</sup> , Luiz Emílio Pessoa Timeni de Moraes Filho<sup>3</sup> , Yêda Medeiros Bastos de Almeida<sup>1</sup>  and Glória Maria Vinhas<sup>1</sup> 

<sup>1</sup>Laboratório de Petroquímica, Departamento de Engenharia Química, Universidade Federal de Pernambuco, Recife, PE, Brasil

<sup>2</sup>Laboratório de Microbiologia, Departamento de Engenharia Química, Universidade Federal de Pernambuco, Recife, PE, Brasil

<sup>3</sup>Chemical Engineering Department, University of Utah, Salt Lake City, Utah, United States of America

\*mifelixsilva@hotmail.com

## Abstract

The use of natural antimicrobial additives, such as orange essential oil (OO), can be a promising possibility to increase food shelf life with the aid of active packaging. This study aimed to develop an active packaging using orange oil and PBAT – poly (butylene adipate co- terephthalate) to store mozzarella cheese produced by a fine film extruder with 5, 10, and 15% OO (w/w). In the results, D-limonene was oil's main constituent with antimicrobial activity against *E. aerogenes*, *E. coli*, and *S. aureus*. The addition of the oil did not alter the thermal stability of the film. The water vapor permeability increased with increasing oil concentration. All films presented high strength. However, films with higher OO concentrations favored the degradation process, as observed in the activation energy. The active packaging added with 15% OO (PBAT15) was efficient, reducing microbial growth up to 6 days of storage of mozzarella cheese.

**Keywords:** antimicrobial, orange oil, PBAT, active packaging.

**How to cite:** Andrade, M. F., Silva, I. D. L., Caetano, V. F., Silva, G. A., Moraes Filho, L. E. P. T., Almeida, Y. M. B., & Vinhas, G. M. (2023). Active antimicrobial extruded films for mozzarella cheese from PBAT and orange oil. *Polímeros: Ciência e Tecnologia*, 33(2), e20230017. <https://doi.org/10.1590/0104-1428.20220112>

## 1. Introduction

Food packaging has essential functions: protection, communication, convenience, and containment. In addition to these, they preserve food from external contamination, maintain freshness and quality, and when possible, extend the shelf life of food<sup>[1]</sup>. Active packaging has, in addition to the characteristics of conventional packaging, the ability to preserve or control the quality of packaged foods<sup>[2]</sup>. The development of active packaging that provides longer shelf lives and improves food quality and safety is one of the most challenging research activities<sup>[3]</sup>.

Furthermore, the antimicrobial additives inserted in the packaging increase the interaction between packaging and food by decreasing deterioration by microorganisms and reducing the growth of pathogens<sup>[3]</sup>. Promising additives for the use of antimicrobial agents are essential oils extracted from plants. Numerous essential oils are classified by the Food and Drug Administration (FDA) as Generally Recognized as Safe (GRAS) and present antimicrobial, medicinal, biocide, and other activities<sup>[4]</sup>.

Orange essential oil (OO) can be extracted mainly from the peel and the leaves. Its composition is extensive, but terpenoids (monoterpenes) are the main constituents with about 85-99% of the composition. Generally,

the main compound is limonene, and its concentration can reach over 90%<sup>[5]</sup>.

For the production of antimicrobial packaging, poly (butylene adipate co-terephthalate) (PBAT) was used with the possibility of producing active and biodegradable packages. PBAT (Ecoflex) is an aliphatic-aromatic copolyester, biodegradable and has properties similar to low-density polyethylene (LDPE) due to its high molecular weight and branched molecular structure<sup>[6]</sup>, it has high flexibility, impact resistance, easy processability and melting point around 120 °C<sup>[7]</sup>.

Hence, the main objective of this study was to evaluate the properties of PBAT films and orange essential oil obtained by the extrusion of thin films and their application for the protection of mozzarella cheese.

## 2. Materials and Methods

### 2.1 Materials

For the development of the research, PBAT Polymer – Acquired by BASF (Germany), with the trade name ECOFLEX® F BLEND C1200, and the orange essential oil (OO) of *Agroterenas* (São Paulo, Brazil) were used.

## 2.2 Production of the PBAT/OO films

The films were prepared by Lab-16 Chill roll from AX PLÁSTICOS (São Paulo, Brazil). It is a single-screw extruder equipped with a flat die. Initially, 200 g of PBAT was used and the three concentrations of OO (5, 10, and 15% (w/w)) were formulated. The samples were named PBAT5, PBAT10, and PBAT15, according to the concentration of the samples.

## 2.3 Gas chromatography-mass spectrometry (GC-MS) of OO

GC-MS analysis was used to identify and quantify the components present in OO and was performed using a Trace 1300, Thermo Xcalibur Instrument Chromatograph (Massachusetts, USA), with a capillary column TGMS-5 (5% phenyl/95% dimethylpolysiloxane). The analysis lasted approx. 18.00 min, the temperature programming was 60 °C/min, heating rate of 6 °C/min until 100 °C, then of 14 °C/min until 260 °C.

## 2.4 Disc-diffusion analysis on agar of OO

To confirm antimicrobial activity, OO was submitted to a disk-diffusion test in agar to obtain the diameter of the inhibition halo. The test followed the methodology proposed by<sup>[8]</sup> with adaptations. The bacteria used for the test were *Escherichia coli*, *Enterobacter aerogenes*, and *Staphylococcus aureus* and the test was performed in duplicate. The oil was analyzed without dilution and measurements of the halo diameter were performed at 24 and 48 hours.

## 2.5 Colorimetric assay and transparency

The resulting color of the films was determined by a Color View BYK colorimeter (Germany). The samples were placed on white support and the values obtained were compared with standard data, according to Arrieta et al.<sup>[9]</sup> with adaptations. The values are expressed as the average triplicates of each formulation. The results are expressed as L (Metric luminosity), a (Red axis (+) to green (-)), b (Yellow axis (+) to blue (-)), and ΔE (Color difference).

The Transparency (T) of the films was obtained in an Edutec Spectrometer (São Paulo, Brazil) from the measurement of the transmittance of the films at the wavelength of 600 nm<sup>[10]</sup>.

## 2.6 Fourier-transform infrared spectroscopy (FTIR) and Principal component analysis (PCA)

The absorption spectra in the infrared region of the oil, PBAT, and films were performed in Spectrum 400 PerkinElmer equipment (United States) and were obtained in the region of 4000- 650 cm<sup>-1</sup> in absorbance mode, with 16 scans and a resolution of 4 cm<sup>-1</sup> at a temperature of approximately 22 °C and HATR accessory<sup>[11]</sup>. The spectra obtained by FT-IR were analyzed by Principal Component Analysis (PCA), using The Unscrambler 9.7. The spectrum analysis region was in the range of 3200 to 650 cm<sup>-1</sup>, with Standard Normal Variate as a pre-processing technique<sup>[12]</sup>.

## 2.7 Thermal analysis – DSC and TGA

Exploratory differential calorimetry (DSC) was performed in a ISTAR e System, Mettler Toledo equipment (Sao Paulo, Brazil) under a nitrogen atmosphere (50 mL/min).

The samples were cut and weighed with approximately 6 mg, and then sealed in aluminum crucibles. All samples were submitted to three ramps: 0 to 200 °C with 30 °C/min. The second ramp ranged from 200 to 0 °C and the third stage from 0 to 200 °C, with a temperature change ratio of 10 °C/min<sup>[13]</sup>.

Thermogravimetric analysis (TGA) was performed in Shimadzu DTG 60H equipment (Kyoto, Japan), under heating from 35 to 550 °C and a heating rate of 20 °C/min, and the flow of 20 mL/min of nitrogen and sample mass of approximately 20 mg.

## 2.8 Water vapor permeability (WVP)

In a desiccator, a saturated solution of sodium chloride (75% RH) was prepared. In a Becker with a 4.4 cm diameter, dry calcium chloride (dried at 100 °C for 72 hours) was added up to a certain height so that there was 1.5 cm between the salt and the Becker opening. The film was sealed with adhesive tape on the surface of the beaker. Weight changes in the system were measured for 10 days every 24 hours.

Water vapor transmission rate (WVTR) and water vapor permeability (WVP) were calculated from Equations 1 and 2:

$$WVTR = \frac{\Delta m}{\Delta t \times A} \quad (1)$$

$$WVP = \frac{\Delta m}{\Delta t \times A} \times \frac{X}{\Delta P} \quad (2)$$

Where Δm is the weight difference, Δt is the time interval in which Δm was observed, A is the area, X is the mean film thickness (mm) and ΔP is the difference in water vapor pressure between both sides of the film (Pa).

## 2.9 Thickness and mechanical tensile test

The thicknesses of the samples were obtained from the average of 3 points per film in 7 films per formulation, totaling 21 points. A Mitutoyo micrometer with a precision of 0.01 mm was used.

The mechanical tensile test followed the ASTM D882-10 standard for films<sup>[14]</sup>. Tests were performed at room temperature, using universal testing equipment EMIC DL500, at a speed of 50 mm/min, with a load cell of 20 N. The dimensions of the specimens were 10 cm long by 1 cm wide. Seven samples per formulation were used.

## 2.10 Statistical analysis

Statistical data were analyzed through analysis of variance (ANOVA) using STATISTICA software, version 10.0.228.8. The Duncan test was used to determine the difference in significance level of 5% (p ≤ 0.05)

## 2.11 Antimicrobial activity of active packaging for mozzarella cheese

Antimicrobial activity tests followed the methodology described by Dannenberg et al.<sup>[15]</sup>. The test was performed in triplicate, with the samples stored in a refrigerator at a temperature of ± 4° C. The test was performed over the course of 13 days.

### 3. Results and Discussions

#### 3.1 Gas chromatography mass spectrometry (GC-MS)

In the OO chromatogram, it was possible to identify 6 components from the intensity of the peaks. In the results, the principal component was the d-limonene (99.5%) is observed with the highest concentration present in OO. The other components of lower concentration are  $\alpha$ -Pinene, Linalool,  $\alpha$ -Phellandrene, Octanal, and Decanal. D-limonene is a monoterpene, volatile and aromatic obtained from the extraction of oil from the orange peel. It presents high antimicrobial, antioxidant, and therapeutic activity<sup>[16]</sup>. It is widely used in various industrial sectors. Its greatest applicability is in the conservation of food. It can be administered orally by humans, presenting rapid absorption in the intestine, easy metabolization, and low toxicity. For these reasons, it is considered a safe compound for consumption<sup>[17]</sup>.

#### 3.2 Disc-diffusion analysis on agar

From the diameter of the halo, it was observed that the OO presented antimicrobial activity for the three microorganisms. For OO, there was a larger inhibition zone for the gram-negative microorganism, *E. coli*, with a diameter of 20.2 mm, while *E. aerogenes* presented a diameter close to that found for gram-positive *S. aureus*: 10.3 and 10.6 mm, respectively.

According to the National Committee for Clinical Laboratory Standards<sup>[18]</sup> the diameters of the halos found in the disc-diffusion test can be classified, as to their activity, as being resistant, to a diameter equal to or less than 14 mm, intermediate, when the diameter is between 15 and 19 mm, and sensitive when the diameters are greater than 20 mm. Thus, OO can be considered sensitive to the Microorganism *E. coli* and resistant to *E. aerogenes* and *S. aureus*.

Essential oils act by compromising the integrity and function of the cell membrane of microorganisms. That is, these oils can alter the functioning of the membrane through a change in potential, leakage of intracellular components, and inhibition of cellular respiration<sup>[19]</sup>. These characteristics are responsible for cell death or growth inhibition.

#### 3.3 Colorimetric assay and transparency

The color of the films is an important parameter for the appearance and acceptance of packaging by the consumer. The values obtained for L, a, b,  $\Delta E$ , and transparency can be observed in Table 1.

For the additivated films, the increase in OO concentration caused significant changes in  $a^*$  and  $b^*$  and an increase in total color difference ( $\Delta E$ ), thus confirming the incorporation

of oil into the polymer matrix. The color difference was significant as the OO content in the samples increased.

Table 1 presents the transparency of films at wavelength 600 nm ( $T_{600}$  for UV light) indicating a decrease in the transparency of films with the addition of OO. Studies indicate that lower values in transparency are related to greater difficulty in light transmission<sup>[20]</sup>.

The films became orange with the increase of oil, which caused a barrier against the light. The incorporation of essential oils causes a decrease in the transparency of films, mainly due to a reduction in light transmission caused by the scattering of light by the oil droplets in the polymer matrix<sup>[21]</sup>. In general, the reduction in transparency will depend on the type of essential oil used.

The use of films of lower transparency for packaging can be useful to reduce food exposure to UV and visible rays, which initiate the degrading process of food<sup>[22]</sup>.

#### 3.4 Fourier Transform Infrared Spectroscopy (FTIR) and Principal Component Analysis (PCA)

The spectra of OO, PBAT, and films with the addition of OO are presented in Figure 1.

The spectrum for OO presents peaks around 1643  $\text{cm}^{-1}$  which can be divided into two absorption frequencies: the first at 1650  $\text{cm}^{-1}$ , which is related to the hydroxyl groups, and the second at 1633  $\text{cm}^{-1}$  to the C=C vibration mode. Furthermore, the following characteristic peaks: 3074 and 3011  $\text{cm}^{-1}$  (stretch vibrations =C-H), 2964 and 2921  $\text{cm}^{-1}$  (Stretch vibrations of the C-H), and those in 1643 and 1676  $\text{cm}^{-1}$  (c=c stretch vibrations), which are related to the ring and the vinyl group, respectively, are present<sup>[23]</sup>.

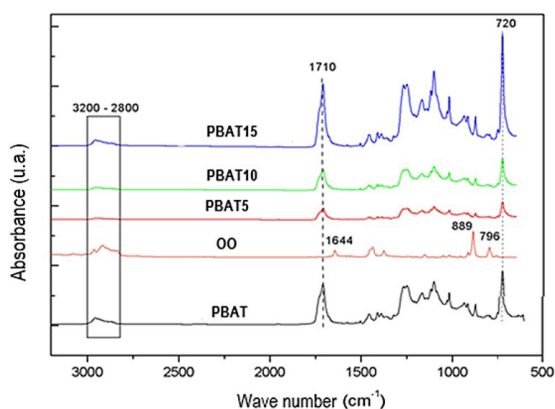


**Figure 1.** FTIR spectrum of PBAT, PBAT5, PBAT10, and PBAT15 films.

**Table 1.** Color and transparency of PBAT, PBAT5, PBAT10, and PBAT15 films.

Samples	L	a	b	$\Delta E$	Transparency (%)
PBAT	97.50 <sup>a</sup> ± 0.14	-0.65 <sup>a</sup> ± 0.02	0.73 <sup>d</sup> ± 0.01	1.61 <sup>d</sup>	6.14 <sup>a</sup> ± 0.19
PBAT5	96.43 <sup>b</sup> ± 0.05	-5.62 <sup>b</sup> ± 0.05	15.09 <sup>c</sup> ± 0.08	16.76 <sup>c</sup>	1.94 <sup>c</sup> ± 0.38
PBAT10	95.55 <sup>d</sup> ± 0.06	-7.98 <sup>c</sup> ± 0.11	24.48 <sup>b</sup> ± 0.42	25.71 <sup>b</sup>	2.27 <sup>b</sup> ± 0.17
PBAT15	96.16 <sup>c</sup> ± 0.08	-8.99 <sup>d</sup> ± 0.01	28.25 <sup>a</sup> ± 0.06	29.52 <sup>a</sup>	0.22 <sup>d</sup> ± 0.50

\*Equal letters in the same column indicate that they are not significantly different by the Duncan Test ( $p \leq 0.05$ ).

All films presented the vibration region of the CH groups (3200 – 2800) and a more intense vibration in the band at 2954 cm<sup>-1</sup> and 2920 cm<sup>-1</sup> (stretch vibration CH<sub>3</sub>, CH<sub>2</sub>, CH). In addition, it is possible to observe a sharper peak at 1710 cm<sup>-1</sup> (C=O of the ester bond) and another at 720 cm<sup>-1</sup> (vibration of the methylene group (CH<sub>2</sub>), characteristic region of PBAT<sup>[24]</sup>.

Analyzing the infrared spectra, it was not possible to observe the appearance of any band characteristic of the presence of OO. This behavior may have occurred because both OO and PBAT have regions with similar characteristic vibrations.

Thus, the PCA technique was performed to verify whether the OO interacted with the vibrational regions of the PBAT. PCA is a multivariate analysis using data collection and thus relates trends from the signal analysis. The results are expressed by the linear combination of vectors, called principal components (PCs), so the PCA converts the data into groups of uncorrelated variables (PCs)<sup>[12]</sup>.

Therefore, principal component analysis was used to verify whether the application of orange oil caused any change in the chemical structure of PBAT, according to Figure 2.

From the graph of Scores PC1xPC2 (Figure 2), it can be observed that the first component (PC1 - horizontal axis) explained 88% of the variability in the spectral information and the second component (PC2 - vertical axis) presented 11% of the variability in the spectral information.

It is possible to observe that the PBAT film, in the PC1 axis (horizontal), lies within the same region as PBAT10. PC1 then was able to identify differences between PBAT15 and PBAT5. PC2, however, was able to identify the differences between PBAT and PBAT10. Hence, the two PCs when plotted together show the formation of 4 groups: one group for the pure PBAT film (P) and three other groups for PBAT films with 5%, 10%, and 15% of OO.

Thus, it can be indicated that, with PC1, it is possible to distinguish between PBAT films with 5 and 15% from the others, while with PC2, it is possible to identify the differences between pure PBAT and PBAT with 10%.

Given the results observed by the PCA, it is possible to suggest that this separation is probably indicative of the presence of orange oil (OO) in the matrix of PBAT films, thus presenting a possible interaction between PBAT and OO.

### 3.5 Thermal analysis: DSC and TGA

The respective values for crystallization and melting temperatures, as well as melting and crystallization enthalpies and crystallinity degree, are displayed in Table 2.

From Table 2 data, it is possible to observe that there was no variation in the crystallization temperature (T<sub>c</sub>) of the samples, with a reduction of only 1 °C for films with 10% OO, as well as there was no change in the values of melting temperature (T<sub>f</sub>). The peak of PBAT fusion can vary in the range of 85 °C to 145 °C<sup>[25]</sup> this wide fusion range of PBAT is due to being a copolymer in blocks formed by repeat units of butylene adipate (BA) and butylene terephthalate (BT), being called flexible segment and rigid segment, respectively<sup>[6]</sup>.

Crystallization enthalpy, crystallinity degrees, and melting enthalpy increased with the addition of the oil, indicating that it probably modified the structure of PBAT, which now required less energy to crystallize and more energy to fuse the polymer.

The increase in fusion enthalpy (ΔH<sub>m</sub>) may be related to the presence of more perfect or larger crystals in the PBAT structure, for this to happen, the OO could act to facilitate the mobility and the packaging of polymeric chains, thus increasing the degree of crystallinity and ΔH<sub>m</sub><sup>[26]</sup>.

The degradation temperatures of all samples occurred in a single step with marked mass loss and that can be observed in Figure 3. The presence of OO did not alter PBAT degradation temperatures.

The values for the initial degradation temperatures (T<sub>onset</sub>), final degradation temperature (T<sub>endset</sub>), maximum degradation temperature (T<sub>deg.max</sub>), and residue are displayed in Table 3.

The degradation temperature of PBAT is in the range of 355-440 °C<sup>[6]</sup>, can be observed that temperatures (T<sub>onset</sub>, T<sub>endset</sub>, and T<sub>deg.max</sub>) there was no noticeable variation in thermal stability, regardless of the concentration of oil added to the samples.

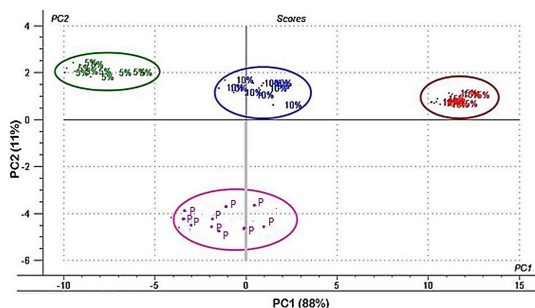


Figure 2. PC1 x PC2 Score Charts for pure PBAT (P) films and PBAT films additivated with 5%, 10%, and 15% OO.

Table 2. Thermal properties by DSC of PBAT, PBAT5, PBAT10, and PBAT15 films.

Sample	Cooling			2nd Heating		
	T <sub>c</sub> (°C)	ΔH <sub>c</sub> (J/g)	X <sub>c</sub> (%)	T <sub>f</sub> (°C)	ΔH <sub>m</sub> (J/g)	X <sub>c</sub> (%)
PBAT	80.03	10.11	8.87	122.82	7.77	6.82
PBAT5	79.51	10.97	9.62	122.73	9.15	8.03
PBAT10	78.99	12.31	10.80	122.85	9.43	8.27
PBAT15	80.53	12.15	10.66	122.99	8.72	7.65

In addition, PBAT does not change its structure at processing temperatures below 200 °C<sup>[27]</sup>. Therefore, the production of the film in an extruder at 180 °C as the processing temperature did not alter the thermal properties of the polymer.

Activation energy is related to the necessary energy to start a reaction. In this case, the degradation reaction. As can be observed, the samples PBAT5 and PBAT10 presented higher  $E_a$  when compared to PBAT, hence, it is necessary for more energy for the degradation process to begin. On the other hand, the sample PBAT15 presented lower activation energy when compared to PBAT, indicating that higher OO concentrations favor the degradation process of PBAT.

### 3.6 Water Vapor Permeability (WVP)

The WVP measures the transport of moisture across the film. This is a crucial parameter for the lifespan of a product. Films that present high permeability may have their application on fresh vegetables, while films with low permeability may be used for dehydrated products. WVP and WVTR may be observed in Table 4.

It is possible to observe that films with the addition of OO presented a slower WVTR when compared to PBAT. Films with 10 and 15% OO presented a significant ( $p \leq 0.05$ ) reduction in WVTR. It is important mentioning that WVTR does not take into account film thickness, but only moisture absorption as a function of time.

For the WVP, there was a significant increase in film permeability. This behavior may be related to the increase in free volume within the polymeric matrix due to the interaction between the additive molecule and the polymeric chain<sup>[28]</sup>.

Therefore, it appears that although films with OO present a lower rate of water absorption over time (WVTR), more water is absorbed by the polymeric chain throughout the test due to the greater thickness of the film, providing an increase in the permeability (WVP) of the films containing OO in relation to the PBAT film.

Overall, it is possible to observe that because of the absence of cracks or visible tears on the surface, water crosses the films through diffusion, moving within the empty spaces present in the polymeric structure.

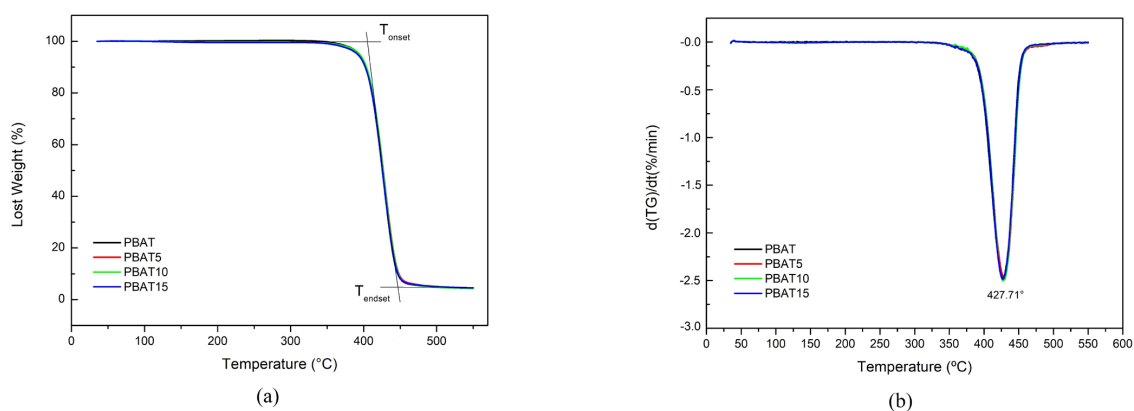


Figure 3. (a) TGA and (b) DTG curves from PBAT, PBAT5, PBAT10, and PBAT15.

Table 3. Degradation temperatures for PBAT, PBAT5, PBAT10 and PBAT15 samples.

Sample	$T_{onset}$ (°C)	$T_{endset}$ (°C)	$T_{deg,max}$ (°C)	Residue (%)	$E_a$ (kJ/mol)
PBAT	401	446	427	4.48	576.31
PBAT5	399	449	428	4.45	593.61
PBAT10	398	449	427	4.31	597.39
PBAT15	399	446	428	4.56	569.08

Table 4. WVTR and WVP for PBAT films additivated with OO.

Sample	Thickness (mm)	WVTR (g/h.m <sup>2</sup> )	WVP (g/h.m.Pa) x 10 <sup>7</sup>
PBAT	0.185 <sup>c</sup> ± 0.002	7.43 <sup>a</sup> ± 1.72	5.79 <sup>c</sup> ± 0.47
PBAT5	0.217 <sup>c,b</sup> ± 0.078	7.05 <sup>a</sup> ± 2.07	7.20 <sup>a</sup> ± 0.50
PBAT10	0.231 <sup>b</sup> ± 0.004	6.58 <sup>b</sup> ± 1.65	6.49 <sup>b</sup> ± 0.48
PBAT15	0.280 <sup>a</sup> ± 0.002	5.91 <sup>c</sup> ± 1.74	7.00 <sup>a</sup> ± 0.32

\*Equal letters in the same column indicate that they are not significantly different by the Duncan Test ( $p \leq 0.05$ ).

### 3.7 Thickness and mechanical tensile test

The results of the thicknesses obtained for the extruded films can be observed in Table 5.

It is possible to see that the addition of the oil caused an increase in the thickness of the films as the oil concentration was increased.

This behavior observed for the thickness may be related to the increase in free volume caused by the interaction of oil in the polymer matrix, which will favor a greater spacing between the chains and, consequently, an increase in thickness.

As Kurt and Kahyaoglu<sup>[29]</sup> affirm, changes in film thicknesses can modify important characteristics such as permeability, transparency, and mechanical properties

From the results shown in Table 5, there was a significant increase in the tension at rupture for films with 10% and 15% OO and a reduction for films with 5% OO. The elongation increased with the addition of the oil. This increase is more significant with the concentration of 10% and 15%. The module did not show linear behavior, as its values decreased in films with 5% and 15% OO and increased significantly in films with 10%.

The increase in tensile strength of films with 10% and 15% OO may be related to the possibility of a structural rearrangement in the polymer matrix caused by the addition of oil, promoting an increase in traction properties<sup>[30]</sup>.

This increase in elongation may be related to the reduction in the aggregation of polymer chains due to the presence of oil, which facilitates the sliding of chains during stretching<sup>[31]</sup>. The values observed for elongation had greater variations than the results obtained from the stress. According to other studies, the elongation of the material suffers greater interferences when compared with tension<sup>[32]</sup>.

An increase in the value of the module for the concentration of 10% is in accordance with the results observed for the degree of crystallinity, in which it was found that 10% presented an  $X_c$  higher than the other concentrations, making the film more rigid. Therefore, it can be emphasized that the concentration of 10% OO was the one that caused the greatest changes in the final physical characteristics of PBAT.

All samples have higher mechanical strength than low-density polyethylene (6.9-16 MPa)<sup>[28]</sup>. The results presented for the films were superior for all samples analyzed, allowing their use as packages that support high stresses.

### 3.8 Application of PBAT15 film as packaging for mozzarella cheese

The microbiological growth of the film/cheese system using the dilution of  $10^{-4}$  CFU (colony forming units) for *E. coli*. and film with 15% OO can be observed in Figure 4.

Analyzing the data from Figure 4, it was verified that the PBAT15 film caused a reduction in microbial growth in the first 6 days of freezer storage. In the first 6 days, there was a reduction of about 65% of the microbial growth of *E. coli* on the surface of mozzarella cheese, although, in the following days, 9 and 13, microorganisms would grow again, but more slowly and with a reduction of about 28% compared to the beginning of the test. These results confirm its antimicrobial potential for application in active packaging for use in mozzarella cheese.

For the PBAT film, it is observed that there was mitigation in microbial growth, which was approximately 20% on days 6 and 9. The contact of PBAT with the surface of the cheese may have chemically modified this surface, such as reducing moisture, making microbial proliferation slower.

According to Sung et al.<sup>[33]</sup> the vast majority of the extracts and/or oils extracted from plants have a high sensitivity to film processing conditions. This is because, when subjected to certain temperature and pressure conditions, antimicrobials can evaporate in an accelerated manner.

In addition, the interactions that can occur both between the polymer matrix and the additive and between the additive and the composition of the food can alter the efficiency of the active packaging<sup>[34]</sup>. Among these factors are: pH, presence of moisture, fat, protein content, additives, solutions, storage temperature, and composition of the atmosphere<sup>[35]</sup>.

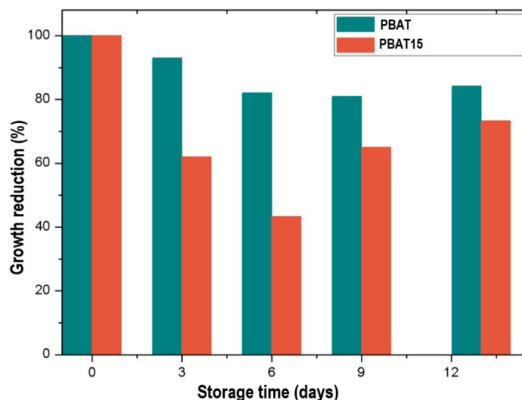


Figure 4. Percentage of microbial growth reduction as a function of storage days for PBAT and PBAT15 films.

Table 5. Thickness and Mechanical Properties of PBAT, PBAT5, PBAT10, and PBAT15.

Samples	Thickness (mm)	Tension at break (MPa)	Elongation at break (%)	Elastic module (MPa)
PBAT	0.185 <sup>c</sup> ± 0.002	32.16 <sup>c</sup> ± 0.72	950.90 <sup>c</sup> ± 21.46	68.11 <sup>b</sup> ± 2.07
PBAT5	0.217 <sup>b,c</sup> ± 0.078	27.83 <sup>d</sup> ± 1.05	955.78 <sup>c</sup> ± 17.81	66.01 <sup>b,c</sup> ± 1.24
PBAT10	0.231 <sup>b</sup> ± 0.004	33.99 <sup>b</sup> ± 1.38	1073.40 <sup>b</sup> ± 24.87	74.75 <sup>a</sup> ± 1.96
PBAT15	0.280 <sup>a</sup> ± 0.002	35.68 <sup>a</sup> ± 0.80	1177.6 <sup>a</sup> ± 18.91	63.42 <sup>c</sup> ± 2.39

\*Equal letters in the same column indicate that they are not significantly different by the Duncan Test (p<0.05).

## 4. Conclusions

It was possible to produce films from PBAT and orange essential oil by extrusion and confirmed the incorporation of the oil in the polymeric matrix. The films remained resistant enabling their use as packaging. Thus, it can be concluded that there was incorporation and migration of orange oil from the polymer matrix, confirming its potential as an active packaging for food.

## 5. Author's Contribution

- **Conceptualization** – Michelle Félix de Andrade; Gloria Maria Vinhas.
- **Data curation** – Michelle Félix de Andrade; Ivo Diego de Lima Silva; Viviane Fonseca Caetano.
- **Formal analysis** – Michelle Félix de Andrade.
- **Funding acquisition** - Yêda Medeiros Bastos de Almeida; Glória Maria Vinhas.
- **Investigation** – Michelle Félix de Andrade; Ivo Diego de Lima Silva.
- **Methodology** – Michelle Félix de Andrade; Gisely Alves da Silva; Viviane Fonseca Caetano.
- **Project administration** – Michelle Félix de Andrade; Yêda Medeiros Bastos de Almeida; Glória Maria Vinhas.
- **Resources** – Yêda Medeiros Bastos de Almeida; Glória Maria Vinhas.
- **Software** – Luíz Emílio Pessoa Timeni de Moraes Filho.
- **Supervision** – Yêda Medeiros Bastos de Almeida; Glória Maria Vinhas.
- **Validation** – NA.
- **Visualization** – NA.
- **Writing – original draft** – Michelle Félix de Andrade.
- **Writing – review & editing** – Michelle Félix de Andrade; Luiz Emílio Pessoa Timeni de Moraes Filho.

## 6. Acknowledgements

This work was supported by the CNPq - National Council for Scientific and Technological Development (158667/2018-2) and FACEPE - Foundation for Support of Science and Technology of the State of Pernambuco (BFP-0151-3.06/20).

## 7. References

1. Siracusa, V., & Lotti, N. (2019). *Intelligent packaging to improve shelf life*. In C. M. Galanakis (Ed.), *Food quality and shelf life* (pp. 261-279). UK: Academic Press. <http://dx.doi.org/10.1016/B978-0-12-817190-5.00008-2>
2. Khumkomgool, A., Saneluksana, T., & Harnkarnsujarit, N. (2020). Active meat packaging from thermoplastic cassava starch containing sappan and cinnamon herbal extracts via LLDPE blown-film extrusion. *Food Packaging and Shelf Life*, 26, 100557. <http://dx.doi.org/10.1016/j.fpsl.2020.100557>.
3. Gaglio, R., Botta, L., Garofalo, G., Miceli, A., Settanni, L., & Lopresti, F. (2021). Carvacrol activated biopolymeric foam: an effective packaging system to control the development of spoilage and pathogenic bacteria on sliced pumpkin and melon. *Food Packaging and Shelf Life*, 28, 100633. <http://dx.doi.org/10.1016/j.fpsl.2021.100633>.
4. Costa, R. C., Daitx, T. S., Mauler, R. S., Silva, N. M., Miotto, M., Crespo, J. S., & Carli, L. N. (2020). Poly (hydroxybutyrate-co-hydroxyvalerate)-based nanocomposites for antimicrobial active food packaging containing oregano essential oil. *Food Packaging and Shelf Life*, 26, 100602. <http://dx.doi.org/10.1016/j.fpsl.2020.100602>.
5. Razola-Díaz, M. D., Guerra-Hernández, E. J., García-Villanova, B., & Verardo, V. (2021). Recent developments in extraction and encapsulation techniques of orange essential oil. *Food Chemistry*, 354, 129575. <http://dx.doi.org/10.1016/j.foodchem.2021.129575>. PMID:33761335.
6. Campos, S. S., Oliveira, A., Moreira, T. F. M., Silva, T. B. V., Silva, M. V., Pinto, A. J., Bilck, A. P., Gonçalves, O. H., Fernandes, I. P., Barreiro, M.-F., Yamashita, F., Valderrama, P., Shirai, M. Y., & Leimann, F. B. (2019). TPCS/PBAT blown extruded films added with curcumin as a technological approach for active packaging materials. *Food Packaging and Shelf Life*, 22, 100424. <http://dx.doi.org/10.1016/j.fpsl.2019.100424>.
7. Shankar, S., & Rhim, J.-W. (2016). Tocopherol-mediated synthesis of silver nanoparticles and preparation of antimicrobial PBAT/silver nanoparticles composite films. *Lebensmittel-Wissenschaft + Technologie*, 72, 149-156. <http://dx.doi.org/10.1016/j.lwt.2016.04.054>.
8. Nibir, Y. M., Sumit, A. F., Akhand, A. A., Ahsan, N., & Hossain, M. S. (2017). Comparative assessment of total polyphenols, antioxidant and antimicrobial activity of different tea varieties of Bangladesh. *Asian Pacific Journal of Tropical Biomedicine*, 7(4), 352-357. <http://dx.doi.org/10.1016/j.apjtb.2017.01.005>.
9. Arrieta, M. P., López, J., Ferrándiz, S., & Peltzer, M. A. (2013). Characterization of PLA-limonene blends for food packaging applications. *Polymer Testing*, 32(4), 760-768. <http://dx.doi.org/10.1016/j.polymeresting.2013.03.016>.
10. Han, J. H., & Floros, J. D. (1997). Casting antimicrobial packaging films and measuring their physical properties and antimicrobial activity. *Journal of Plastic Film & Sheeting*, 13(4), 287-298. <http://dx.doi.org/10.1177/875608799701300405>.
11. Dias, M. V., Medeiros, H. S., Soares, N. F. F., Melo, N. R., Borges, S. V., Carneiro, J. D. S., & Pereira, J. M. T. A. K. (2013). Development of low-density polyethylene films with lemon aroma. *Lebensmittel-Wissenschaft + Technologie*, 50(1), 167-171. <http://dx.doi.org/10.1016/j.lwt.2012.06.005>.
12. Petrov, O. V., Lang, J., & Vogel, M. (2021). Exploring the potential of PCA-based quantitation of NMR signals in T1 relaxometry. *Journal of Magnetic Resonance (San Diego, Calif.)*, 326, 106965. <http://dx.doi.org/10.1016/j.jmr.2021.106965>. PMID:33774383.
13. Chivrac, F., Kadlecová, Z., Pollet, E., & Avérous, L. (2006). Aromatic copolyester-based nano-biocomposites: elaboration, structural characterization and properties. *Journal of Polymers and the Environment*, 14(4), 393-401. <http://dx.doi.org/10.1007/s10924-006-0033-4>.
14. American Society for Testing and Materials – ASTM. (2010). *ASTM D882-10: standard test method for tensile properties of thin plastic sheeting*. West Conshohocken: ASTM.
15. Dannenberg, G. S., Funck, G. D., Cruxen, C. E. S., Marques, J. L., Silva, W. P., & Fiorentini, A. M. (2017). Essential oil from pink pepper as an antimicrobial component in cellulose acetate film: potential for application as active packaging for sliced cheese. *Lebensmittel-Wissenschaft + Technologie*, 81, 314-318. <http://dx.doi.org/10.1016/j.lwt.2017.04.002>.
16. Alehosseini, E., Jafari, S. M., & Tabarestani, H. S. (2021). Production of D-limonene-loaded Pickering emulsions stabilized by chitosan nanoparticles. *Food Chemistry*, 354, 129591. <http://dx.doi.org/10.1016/j.foodchem.2021.129591>. PMID:33756315.

17. Vieira, A. J., Beserra, F. P., Souza, M. C., Totti, B. M., & Rozza, A. L. (2018). Limonene: aroma of innovation in health and disease. *Chemo-Biological Interactions*, 283, 97-106. <http://dx.doi.org/10.1016/j.cbi.2018.02.007>. PMID:29427589.
18. Clinical and Laboratory Standards Institute – CLSI. (2018). *M02 - Performance Standards for Antimicrobial Disk Susceptibility Tests*. USA: CLSI.
19. Greay, S. J., & Hammer, K. A. (2015). Recent developments in the bioactivity of mono- and diterpenes: anticancer and antimicrobial activity. *Phytochemistry Reviews*, 14(1), 1-6. <http://dx.doi.org/10.1007/s11101-011-9212-6>.
20. Limpan, N., Prodpran, T., Benjakul, S., & Prasarnpran, S. (2010). Properties of biodegradable blend films based on fish myofibrillar protein and polyvinyl alcohol as influenced by blend composition and pH level. *Journal of Food Engineering*, 100(1), 85-92. <http://dx.doi.org/10.1016/j.jfoodeng.2010.03.031>.
21. Atarés, L., Pérez-Masiá, R., & Chiralt, A. (2011). The role of some antioxidants in the HPMC film properties and lipid protection in coated toasted almonds. *Journal of Food Engineering*, 104(4), 649-656. <http://dx.doi.org/10.1016/j.jfoodeng.2011.02.005>.
22. Adilah, A. N., Jamilah, B., Noranizan, M. A., & Hanani, Z. A. N. (2018). Utilization of mango peel extracts on the biodegradable films for active packaging. *Food Packaging and Shelf Life*, 16, 1-7. <http://dx.doi.org/10.1016/j.fpsl.2018.01.006>.
23. Mallardo, S., De Vito, V., Malinconico, M., Volpe, M. G., Santagata, G., & Di Lorenzo, M. L. (2016). Poly (butylene succinate)-based composites containing  $\beta$ -cyclodextrin / D-limonene inclusion complex. *European Polymer Journal*, 79, 82-96. <http://dx.doi.org/10.1016/j.eurpolymj.2016.04.024>.
24. Kijchavengkul, T., Auras, R., Rubino, M., Alvarado, E., Montero, J. R. C., & Rosales, J. M. (2010). Atmospheric and soil degradation of aliphatic-aromatic polyester films. *Polymer Degradation & Stability*, 95(2), 99-107. <http://dx.doi.org/10.1016/j.polymdegradstab.2009.11.048>.
25. Shahlari, M., & Lee, S. (2012). Mechanical and morphological properties of poly (butylene adipate-co-terephthalate) and Poly (lactic acid) blended with organically modified silicate layers. *Polymer Engineering and Science*, 52(7), 1420-1428. <http://dx.doi.org/10.1002/pen.23082>.
26. Göksen, G., Fabra, M. J., Pérez-Cataluña, A., Ekiz, H. I., Sanchez, G., & López-Rubio, A. (2021). Biodegradable active food packaging structures based on hybrid cross-linked electrospun polyvinyl alcohol fibers containing essential oils and their application in the preservation of chicken breast fillets. *Food Packaging and Shelf Life*, 27, 100613. <http://dx.doi.org/10.1016/j.fpsl.2020.100613>.
27. Al-Itry, R., Lamnawar, K., & Maazouz, A. (2012). Improvement of thermal stability, rheological and mechanical properties of PLA, PBAT and their blends by reactive extrusion with functionalized epoxy. *Polymer Degradation & Stability*, 97(10), 1898-1914. <http://dx.doi.org/10.1016/j.polymdegradstab.2012.06.028>.
28. Gao, S., Zhai, X., Wang, W., Zhang, R., Hou, H., & Lim, L. (2022). Material properties and antimicrobial activities of starch/PBAT composite films incorporated with  $\epsilon$ -polylysine hydrochloride prepared by extrusion blowing. *Food Packaging and Shelf Life*, 32, 100831. <http://dx.doi.org/10.1016/j.fpsl.2022.100831>.
29. Kurt, A., & Kahyaoglu, T. (2014). Characterization of a new biodegradable edible film made from salep glucomannan. *Carbohydrate Polymers*, 104, 50-58. <http://dx.doi.org/10.1016/j.carbpol.2014.01.003>. PMID:24607159.
30. Atarés, L., & Chiralt, A. (2016). Essential oils as additives in biodegradable films and coatings for active food packaging. *Trends in Food Science & Technology*, 48, 51-62. <http://dx.doi.org/10.1016/j.tifs.2015.12.001>.
31. Bonilla, J., Atarés, L., Vargas, M., & Chiralt, A. (2012). Effect of essential oils and homogenization conditions on properties of chitosan-based films. *Food Hydrocolloids*, 26(1), 9-16. <http://dx.doi.org/10.1016/j.foodhyd.2011.03.015>.
32. Oliveira, V. M., Ortiz, A. V., Del Mastro, N. L., & Moura, E. A. B. (2009). The influence of electron-beam irradiation on some mechanical properties of commercial multilayer flexible packaging materials. *Radiation Physics and Chemistry*, 78(7-8), 553-555. <http://dx.doi.org/10.1016/j.radphyschem.2009.03.041>.
33. Sung, S., Sin, L. T., Tee, T., Bee, S., & Rahmat, A. R. (2014). Effects of Allium sativum essence oil as antimicrobial agent for food packaging plastic film. *Innovative Food Science & Emerging Technologies*, 26, 406-414. <http://dx.doi.org/10.1016/j.ifset.2014.05.009>.
34. Gómez-Estaca, J., López de Lacey, A., López-Caballero, M. E., Gómez-Guillén, M. C., & Montero, P. (2010). Biodegradable gelatin-chitosan films incorporated with essential oils as antimicrobial agents for fish preservation. *Food Microbiology*, 27(7), 889-896. <http://dx.doi.org/10.1016/j.fm.2010.05.012>. PMID:20688230.
35. Otero, V., Becerril, R., Santos, J. A., Rodríguez-Calleja, J. M., Nerín, C., & García-López, M.-L. (2014). Evaluation of two antimicrobial packaging films against Escherichia coli O157: H7 strains in vitro and during storage of a Spanish ripened sheep cheese (Zamorano). *Food Control*, 42, 296-302. <http://dx.doi.org/10.1016/j.foodcont.2014.02.022>.

Received: Dec. 05, 2022

Revised: May 04, 2023

Accepted: June 06, 2023